State-and-Evolution Detection Models: A Framework for Continuously Monitoring Landscape Pattern Change

Lingwen Tian, Xiangnan Liu, Meiling Liu, and Ling Wu

***Abstract*— Detecting the evolution of large-area landscape patterns using long-term remote-sensing images is helpful in supporting research on the relationship between landscape patterns and ecological processes, as well as the development of ecological process simulations and spatiotemporal interaction models. However, detection methods have generally been developed as separate applications, each with a separate type of landscape pattern change; remote-sensing images are acquired at epochal timesteps. Consequently, in practical applications, many omission changes for some types of pattern changes and inaccurate evolution time are presented in the detected map. In this article, state-and-evolution detection models (SEDMs) are promoted to obtain complete information about the evolution of landscape patterns based on yearly land cover data. In the proposed framework, we first define the major categories of landscape pattern changes to comprehensively reveal the characteristics of landscape pattern changes associated with real change cases. Next, a morphological rule-based pattern recognition approach is proposed for quantitative discrimination among these categories. This approach is then applied in annual land cover data to continuously detect landscape pattern evolution processes and evolution time. Finally, the detected evolution time in different evolution processes is applied to measure the timestep between two disparate types. The performances of the SEDMs are presented by Landsat-derived land cover evolution in Shanxi, China. The detected results are indirectly verified by the land cover conversion matrix and connect index, indicating strong robustness and generalization ability of the SEDMs.**

***Index Terms*— Continuous, land cover data, landscape pattern evolution, state-and-evolution detection models (SEDMs).**

I. Introduction

A LANDSCAPE is a heterogeneous land area containing multiple ecosystems or a mosaic of different land use/cover [1]. The types, proportions, and spatial arrangements of the landscape ecosystems or land use/cover [2]–[4]—often known as the landscape pattern—are considerably influenced by nature and humans, which may influence ecologic processes and the resulting biodiversity, with profound effects on the ecological, social, and economic functions of systems [5], [6]. The change in the landscape pattern contains meaningful regularity from heterogeneous land areas [7], [8]. The regularity is the typical change patterns (trends and spatial distribution regularities) of landscape patterns related to different ecological processes (such as soil erosion, urban sprawl, agricultural mechanization, and vegetation succession), which is significant for exploring factors and mechanisms that produce and control the landscape pattern [9]. The pattern change analysis on a small spatial scale [10]–[14] and within a short time period lacks repeatability, which cannot explain the spatial patterns and processes on larger temporal (decades or longer) and spatial scales (such as regional landscape levels and higher levels). However, these large-scale phenomena are important because most environmental and resource management issues occur on large/medium-scale and large-scale patterns, and processes must be linked with small-scale ones to understand nature [15]. Therefore, numerous studies on landscape pattern change analysis have emerged based on landscape cells (a group of land cover pixels within a given window) using multiple remote-sensing images that support timely and accurate land cover change information [16]–[19].

The analytical strategies adopted in these studies can be categorized into comparative analysis [11], [20], [21] and spatiotemporal dynamic analysis of landscape patterns (SDALP) [2], [4], [22]–[24]. The comparative analysis highlights differences between landscape patterns in different time phases, but seldom obtains the regularity and process of landscape pattern changes [4], making it difficult to reveal the evolution mechanism. The SDALP describes how a landscape evolves and reflects the basic mechanisms governing the process of landscape changes. Therefore, compared with comparative analysis, the SDALP is more dominant and meaningful in pattern-process dynamic studies.

The models for the SDALP have three steps to reveal the change process: 1) classifying the changes of landscape patterns; 2) quantifying the changes of landscape patterns; and 3) determining the temporal scale. The changes of landscape patterns in the models are typically classified as types (i.e., the type of landscape pattern change/CT) associated with two ecological processes: landscape fragmentation (such as forest fragmentation) or expansion (such as urban growth) [23], [25], [26]. For example, a type change tracker model based on forest fragmentation models was developed to quantify and track the degree and evolution of fragmentation over time [24]. Civco *et al.* [21] created an urban growth

Manuscript received December 7, 2020; revised March 28, 2021 and May 10, 2021; accepted June 7, 2021. Date of publication July 7, 2021; date of current version January 14, 2022. This work was supported by the National Natural Science Foundation of China under Grant 41871223. *(Corresponding author: Xiangnan Liu.)*

The authors are with the School of Information Engineering, China University of Geosciences, Beijing 100083, China (e-mail: tlw@cugb.edu.cn; liuxn@cugb.edu.cn; liuml@cugb.edu.cn; wl_19830807@sohu.com).

This article has supplementary downloadable material available at https://doi.org/10.1109/TGRS.2021.3088537, provided by the authors.

Digital Object Identifier 10.1109/TGRS.2021.3088537

model to quantify and categorize urban changes. These models have generally been developed for a specific application of detecting limited CTs. However, different types of ecological processes usually exist in the same region, covering various combinations of CTs. Therefore, a unified model is needed to detect multiple CTs for the SDALP.

Landscape patterns can be quantified for categorical maps by a series of landscape indices (such as the proportion and configuration of patches, the distribution of patch sizes, and the shape and connectivity of edges) that inform specific spatial characteristics of patches, classes of patches, or entire landscape [27], [28]. Landscape indices are an effective avenue for describing spatial land-use heterogeneity and spatial morphological characteristics, which have been increasingly applied to the analysis of land-use dynamics and landscape pattern change processes [29], [30]. The models for the SDALP track different landscape patterns by using the landscape indices (proportions and continuity of patches) to set thresholds. For a specific CT, its spatial morphological characteristics change little and can be calculated by fewer landscape indices. Therefore, a comprehensive characterization of landscape pattern dynamics requires a change detection model that can detect more spatial morphological features, which means that there is a need to explore suitable combinations of landscape indices for quantifying all kinds of pattern dynamics on a long-term period.

The temporal scale of the SDALP is usually set to epochal timesteps, such as five years [31], decadal [32], or longer [33]. Large temporal scales lack the detailed information of the process. The evolution of CTs cannot be well characterized with multiple-temporal images, because the spatiotemporal discontinuity of the multiple-temporal images causes their limited capacity to detect the time and the process of new CT generation following disturbance (i.e., evolution) [34], [35]. For example, forest fragmentation can vary over time with the interaction of disturbance and recovery processes, thereby altering the amount and spatial configuration of forest patches on a landscape [34]–[36]; the time when forest fragmentation occurs and the related recovery processes cannot be accurately detected based on large temporal scales. Remotely sensed time series data provide consecutive measurements of landscape conditions, allowing the capture of both abrupt and gradual changes over time [37]. Recent landscape pattern change analysis based on remote-sensing time series images has provided more important characteristics of long-term spatial dynamics. For example, Xiao *et al.* [18] detected the spatiotemporal dynamics of the landscape structure in the middle reach of the Heihe River basin from 1990 to 2015 using status and trend indicators. Hermosilla *et al.* [36] described and quantified various forest patterns and temporal trends that emerged in areas following stand-replacing (harvest and wildfire) and non-stand-replacing (such as water stress and insects) disturbances using yearly Landsat data from 1984 to 2016. However, these characteristics are represented as the change turning point and the change trends before and after this point in the single- or multiple-landscape indices' time series related to one ecological process. The categorical CT and evolution in landscape patterns are not considered, thereby limiting the processes of landscape pattern change for land cover to be fully explored.

In this study, we proposed a new framework of detecting the evolution of common types of landscape pattern change based on annual land cover data to improve the detection accuracy and usability in the SDALP. Our proposed state-and-evolution detection models (SEDMs) have two objectives: 1) to comprehensively summarize CTs and 2) to detect the evolution information related to CTs. First, six main CTs associated with important ecological processes are defined based on literature. Then, a discrimination approach is constructed to distinguish these CTs based on four landscape indices and implemented with land cover data using year-by-year recognition strategies to detect the evolution patterns and time. Finally, the timestep between two CTs is calculated based on the detected evolution time. To assess the performance and accuracy of our proposed framework, SEDMs were applied to cropland landscapes as a case study by using annual Landsat land cover data. The output results are validated using the land cover conversion matrix and connect index.

II. Methodology

The proposed SEDM framework comprises three components (Fig. 1) and is performed in MATLAB (V2018a). For most approaches used in spatially explicit landscape modeling, it is common to analyze landscape change across a grid that divides a larger area into smaller regularly sized landscape cells, although they can be any shape and size [38], [39]. Similarly, the first step in building an SEDM is to partition landscape spatially into a set L of n regular cells. An SEDM represents changes over time in state of each cell as a stochastic continuous-time process $\{X_t: t \geq 0\}$, where the state denotes the type of landscape pattern change (CT) at a certain phase; the state space (SS) is a set consisting of k discrete state types ($X_t \in$ SS); t is discrete timesteps [Fig. 1(a)].

A. Defining the State Space Set

The state types captured by SEDMs are the CTs related to typical ecological processes. These processes are generally divided into landscape fragmentation, landscape expansion, and landscape aggregation [4], [22], [25], [36], [40]. Landscape fragmentation (such as forest disturbance) refers to the reduction or segmentation of patches into smaller and independent patches driven by natural (such as fire and insects) or artificial (such as harvesting) processes [Fig. 2(a)] [41]–[43]. Landscape expansion is the increased patch areas of different patch types in landscape [Fig. 2(b)], including soil erosion, desertification, species spreading, urban growth, and forest restoration [23], [44], [45]. Landscape aggregation refers to an increase in nodes between patches (connectivity) and area [Fig. 2(b)], such as forest restoration process. We considered all these three ecological processes in SEDMs.

Six steps of landscape fragmentation are distinguished [Fig. 2(a)] according to spatial morphological rules [25], [46]. In fact, stages are not strictly separated from each other since several of them occur simultaneously; however, the dominant stage can often be identified [25]. For example, dissipation

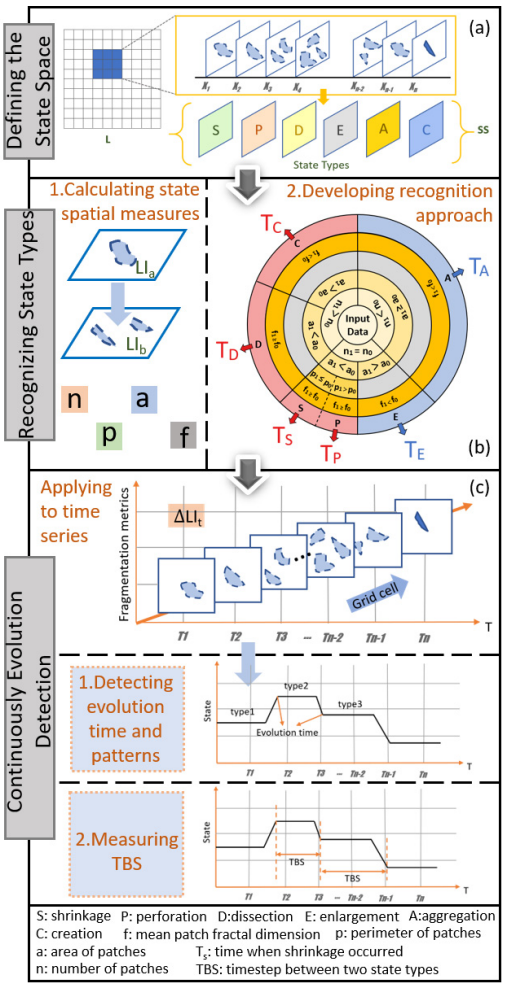

Fig. 1. Flowchart of the proposed SEDM framework. (a) Defining the state space. (b) Recognizing state types. (c) Continuously evolution detection.

stages geometrically have no separate meaning relative to dissection and shrinkage, but it can be regarded as a combined type of dissection and shrinkage. Incision stages can be considered as the same type with dissection stages because of their morphological similarity, although they have different degrees of fragmentation. Likely, attrition stages are similar with shrinkage stages. Shrinkage stages (edge fragmentation) and perforation stages have been identified as two types of forest fragmentation in many studies [22], [26], [40]. Therefore, we summarize three main state types of the fragmentation process caused by different factors: dissection (Type D), shrinkage (Type S), and perforation (Type P). Landscape expansion mainly involves three types of spatial patterns [Fig. 2(b)], i.e., outlying, edge expansion, and infilling, while other types are generally the variants or hybrids of these three basic patterns [4]. In our model, outlying is defined as creation type (Type C), and edge expansion and infilling are merged into enlargement types (Type E) as both internal and external additions to the patch edge. Creation (Type C) and enlargement (Type E) describe the state types of landscape expansion. Aggregation (Type A) is also included in the model.

Consequently, six main state types are integrated and identified, and the SS can be obtained as follows:

$$\mathrm{SS} = \{P, D, S, C, E, A\} \tag{1}$$

where P, D, S, C, E, and A represent the six state types of perforation, dissection, shrinkage, creation, enlargement, and aggregation, respectively.

B. Recognizing State Types

After defining state types from three ecological processes, a morphological rule-based pattern recognition approach is promoted to recognize discrete state types based on the differences of spatial morphological characteristics [Fig. 1(b)]. The response to morphological features (i.e., the shape and form of patches for land cover classes) varied for each state type. A single morphological feature (such as area) is insufficient for detecting various state types, as an obvious feature in one state type may be the same in another one. Therefore, more features are used to identify the six state types of land cover classes. In addition, the judgment condition for detecting state type may be the same for different land cover classes. We select effective landscape indices to detect state types for all land cover classes based on the following principles: 1) they could capture the main morphological features of the patches and 2) they could distinguish different state types. For example, the number of patches in type S is persistent, while type C has an increase in the number of patches. Hence, the number of patches could be used as an indicator to distinguish between type S and type C. Similarly, the perimeter of patches could be used to differentiate type S from type P. According to the principles, four indices are selected after comparing the differences of morphological features between state types: number of patches (LI_1), area of patches (LI_2), perimeter of patches (LI_3), and mean patch fractal dimension (LI_4) [47], [48].

LI_1 equals to the number of patches (n_i) included in land cover class i in landscape cells and $\mathrm{LI}_1 \geq 1$

$$\mathrm{LI}_1 = n_i. \tag{2}$$

A higher LI_1 indicates a more fragmented pattern when the area of the landscape cell does not change. LI_2 is the proportion of a given landscape cell occupied by a land cover class

$$\mathrm{LI}_2 = \sum_{j=1}^{n} L_{ij} \tag{3}$$

where j refers to the different patches of a land cover class, and L_{ij} is the area of patch ij. LI_2 is greater than 0 m^2. A larger value of LI_2 indicates a more dominated cover relative to other land cover classes [49]. LI_3 is the perimeter of patch ij, including the length of patch edge and the perimeter of cavity inside

$$\mathrm{LI}_3 = p_{ij}. \tag{4}$$

The value of LI_3 is greater than 0 m. LI_4 could be calculated as follows:

$$\mathrm{LI}_4 = \frac{\left\{\sum_{i=1}^{m}\sum_{j=1}^{n} 2\ln\left(\frac{0.25\mathrm{LI}_3}{\ln \mathrm{LI}_2}\right)\right\}}{N} \tag{5}$$

where N is the number of patches in landscape cells, and m and n are the number of land cover classes in landscape cells

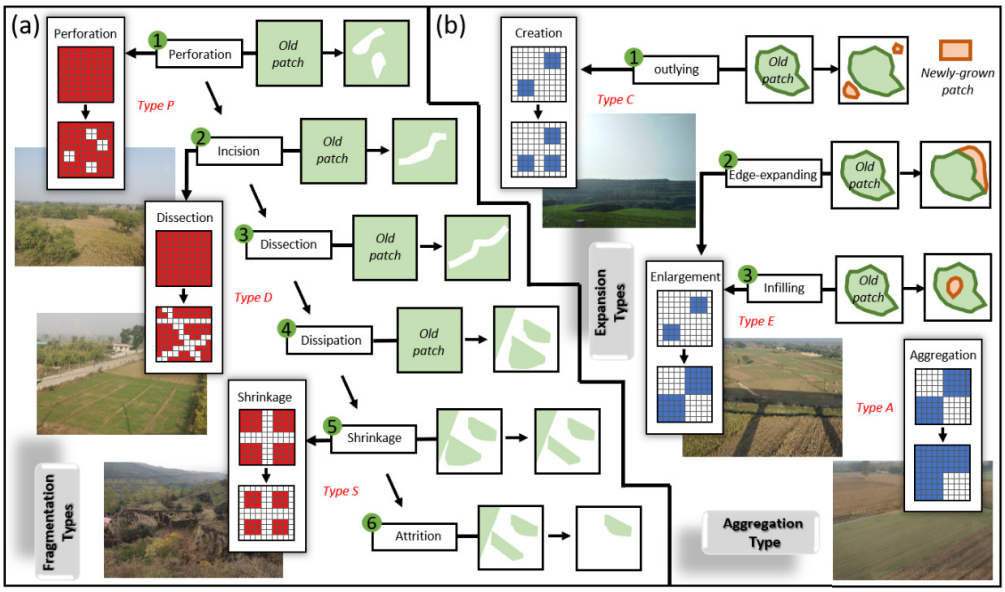

Fig. 2. Types of (a) fragmentation and (b) expansion and aggregation, distinguished according to geometric characteristics.

and the number of patches in a land cover class, respectively. A larger LI_4 value indicates an increase of the complexity of the patch shape (i.e., more fragmentation).

Based on the differences of the four landscape indices between two phases for six state types, a morphological rule-based pattern recognition approach is conducted [Fig. 1(b)] and Fig. 3). For each landscape cell, a and b can present any two phases in state time series

$$X_a = \{\mathrm{LI}_{ai} | i = 1, 2, 3, 4\} \tag{6}$$

$$X_b = \{\mathrm{LI}_{bi} | i = 1, 2, 3, 4\} \tag{7}$$

where X_a and X_b are the states at phases a and b, respectively; LI_{ai} and LI_{bi} are the four index sets obtained at phases a and b, respectively. States from phase a to b can be expressed and recognized by calculating the differences of landscape indices between the two phases

$$\Delta \mathrm{LI}_i = \mathrm{LI}_{bi} - \mathrm{LI}_{ai} \tag{8}$$

with

$$\mathrm{ST}_{(X_a \to X_b)} = \begin{cases} S, & \text{if } \Delta\mathrm{LI}_1 = 0,\ \Delta\mathrm{LI}_2 < 0,\ \Delta\mathrm{LI}_3 \le 0,\ \Delta\mathrm{LI}_4 \ge 0 \\ P, & \text{if } \Delta\mathrm{LI}_1 = 0,\ \Delta\mathrm{LI}_2 < 0,\ \Delta\mathrm{LI}_3 > 0,\ \Delta\mathrm{LI}_4 \ge 0 \\ D, & \text{if } \Delta\mathrm{LI}_1 > 0,\ \Delta\mathrm{LI}_2 < 0,\ \Delta\mathrm{LI}_4 \ge 0 \\ E, & \text{if } \Delta\mathrm{LI}_1 = 0,\ \Delta\mathrm{LI}_2 > 0,\ \Delta\mathrm{LI}_4 < 0 \\ A, & \text{if } \Delta\mathrm{LI}_1 < 0,\ \Delta\mathrm{LI}_2 \ge 0,\ \Delta\mathrm{LI}_4 < 0 \\ C, & \text{if } \Delta\mathrm{LI}_1 > 0,\ \Delta\mathrm{LI}_2 > 0,\ \Delta\mathrm{LI}_4 < 0 \\ \text{Null}, & \text{otherwise} \end{cases} \tag{9}$$

where $\mathrm{ST}_{(X_a \to X_b)}$ is the state type belonging to phase a to phase b. $\Delta\mathrm{LI}_1$, $\Delta\mathrm{LI}_2$, $\Delta\mathrm{LI}_3$, and $\Delta\mathrm{LI}_4$ are the difference values for the four indices between phase a and phase b, respectively. S, P, D, E, A, and C are the defined state types.

C. Detecting State-Type Evolution Time Continuously

Evolution is a change from one type of landscape pattern change into another one. The evolution of state types in the state time series uses continuous detection based on the morphological rule-based pattern recognition approach [Fig. 1(c)]. The dynamic character added in SEDMs allows it to update the time series once new land cover maps become available, so that the evolution process can be adjusted over time. Given a landscape cell, the discriminant rules [(9)] are applied in landscape indices time series of a land cover class; phase a and phase b are changed to two consecutive time points; ST is the state type belonging to phase b; b is the possible evolution time. Indices in landscape cells satisfying the distinguishing criterion are treated as a state type and assigned the value of state type. The others are treated as unrecognized cells and assigned a value of null.

The basis of the detection method is to continuously compare land cover maps in two consecutive years to detect the evolution of the state type since the limited epochal detection. Since landscape pattern in natural areas (such as lakes) does not change significantly within a short time, state-type evolution is determined if a landscape cell is detected as a new state type in multiple consecutive phases (multiple times). Conversely, the landscape pattern that is most frequently disturbed by humans (such as cropland) generally changes within one year. For those landscapes, if a new state type is found in one phase (one times), the landscape cell may evolve. Therefore, SEDMs use the smallest time scale of landscape pattern evolution that has been normalized by "one times" time criterion to detect all land cover classes. If cells show a new state type for one land cover map, an evolution is identified. The cell and time when new state type is detected are assigned to "evolution class" and "evolution time," respectively; otherwise, land cover maps will be flagged as outliers.

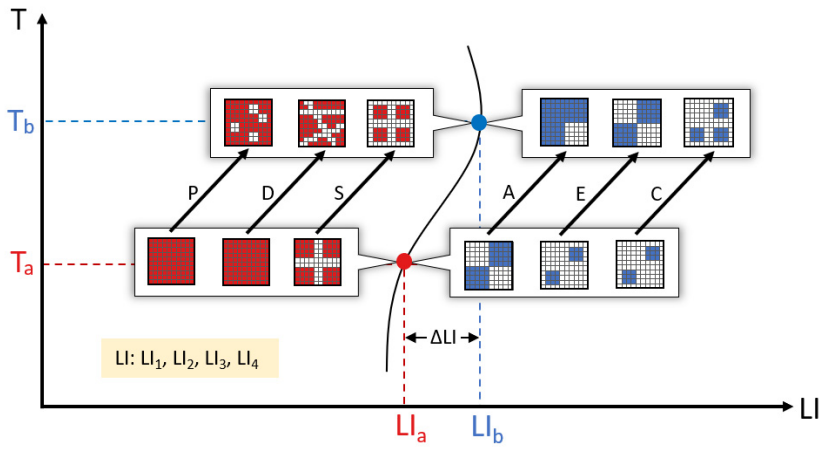

Fig. 3. Sketch map of the state-type discrimination using the morphological-rule-based pattern recognition approach. T_a and T_b are any two phases, LI_a and LI_b are the landscape indices calculated in two phases, and the state type from time T_a to time T_b is judged by the comparing the magnitude of the landscape indices at the two phases.

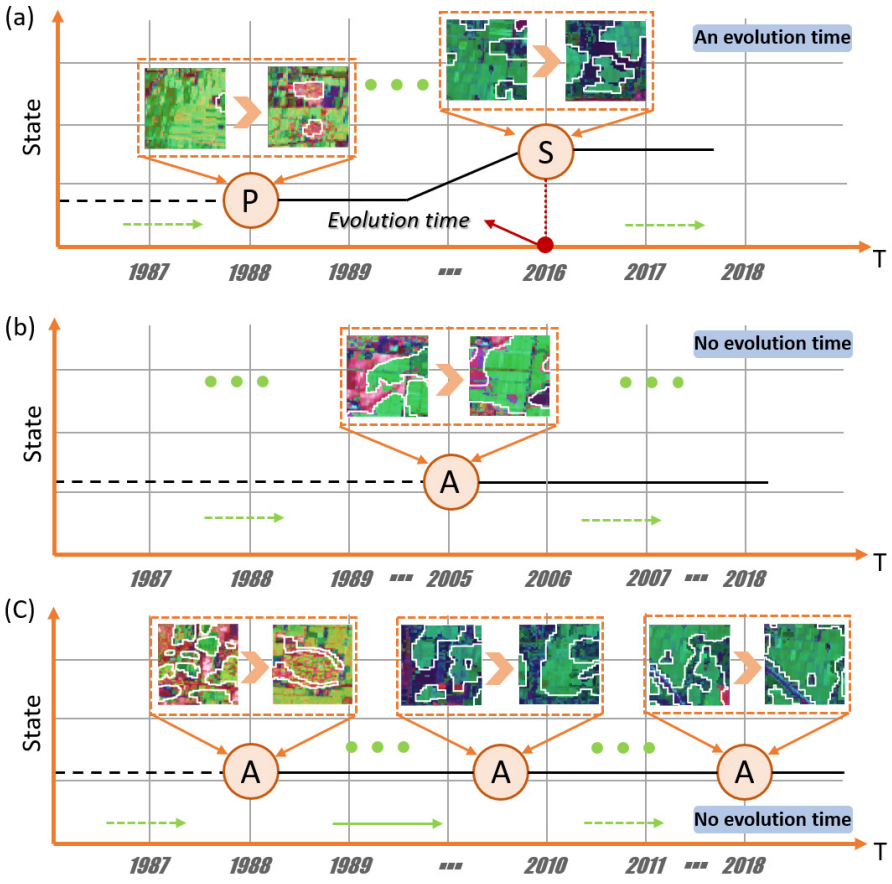

Fig. 4. Example using the threshold of one times and comparison with the former state type for continuous evolution detection. (a) State types and evolution time of a cropland landscape cell generated by SEDMs. (b) and (c) Examples of no evolution time.

Fig. 4(a) illustrates how "one times" time criterion is used to initially detect state-type evolution and time by comparing the present state type and previous one for a cropland landscape cell. When there is no evolution time, one or more land cover maps satisfy the discriminant condition of one state type [Fig. 4(b) and (c)].

D. Tracking State Type Evolution Patterns

In addition to identify evolution time, it is more beneficial to describe the process of state-type evolution [Fig. 1(c)]. The evolved landscape cells have their own state types before and after any evolution time based on the step-by-step evolution detection. By classifying state-type evolution, SEDMs can

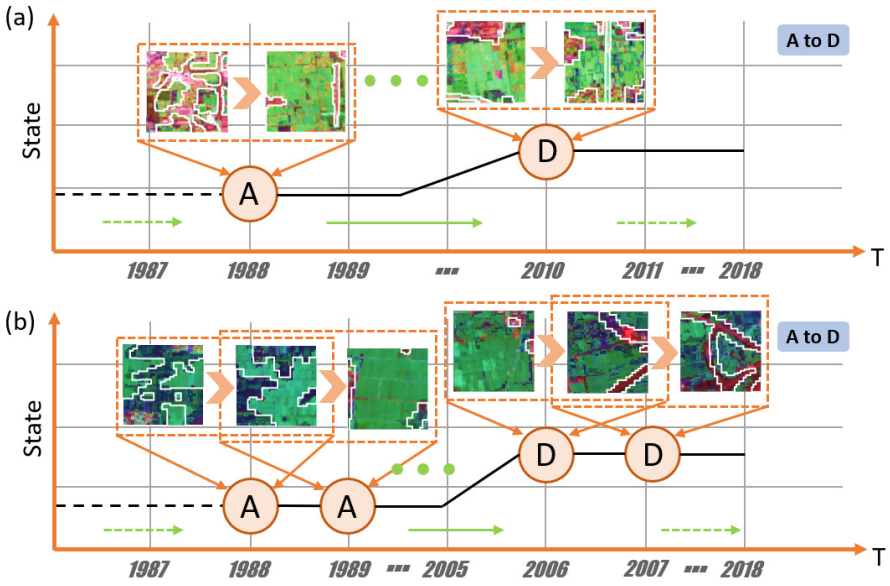

Fig. 5. Two cases of state-type evolution patterns were obtained in two cropland landscape cells. (a) One evolution. (b) Special one evolution.

provide state-type evolution patterns in the entire time period for all landscape cells.

Some principles should be noted when detecting state-type evolution patterns. First, by continuously detecting the time series, only one state type is detected in the landscape cell, which is classified as a "no evolution" pattern [see Fig. 4(b)]. Second, if one evolution is detected, only two state types will be detected during this time period. As shown in Fig. 5(a), the detection results of the time series provide two different state types for a landscape cell, so this cell contains the evolution of "A to D" (A-D). Third, the originally detected state type remains unchanged before a new state type is detected. In Fig. 5(a), the gaps in the two different state types belong to type A because no other state types are detected between these two types. Fourth, if the same state type is detected in a row, it will always be defined as this state type until a different one occurs. For a landscape cell that undergoes an evolution from A to A [Fig. 4(c)], there is no different from the case in the first principle, and it contains merely one state type in the time series. Similarly, although two types of A and D are continuously detected, they still belong to the evolution of A to D since no other types are detected in type A and D [Fig. 5(b)]. These cases demonstrate that the information involved in SEDMs helps to classify the state-type evolution process, and by using the indices' time series, the information can also offer a single state type for a period of unclear evolution.

E. Measuring the Timestep between State Types

Counters are adopted to track the timestep between state (TBS) types for each cell that has undergone evolution [Fig. 1(c)], where TBS represents the timestep to evolve from one state type to another one (Fig. 6). To implement this in the SEDM, the SS for X_t is first improved to include all possible evolution paths (random pairwise combinations of state types) and TBS. To execute counters, each cell is assigned an initial time (T_m) for the first detected state type, and T_m is then updated every timestep (incremented by 1) until a different state type occurs at T_n. TBS is recorded using the follows rules:

$$\text{TBS} = \begin{cases} T_n - T_m, & \text{evolution occurs} \\ 0, & \text{no evolution} \end{cases} \tag{10}$$

The assignment of the cell's TBS depends on whether the cell has an evolution. The time-varying TBS can change with state types, functions of states, and evolution paths. TBS is repeatedly tracked for each evolution path in a similar manner.

III. EXPERIMENTS

In this section, we introduce the input datasets, specify the framework configuring process, and show the output applied in cropland classes in Shanxi, China, including: 1) the evolution pattern output, which records when and where evolution occurs and 2) the TBS output, which records the timestep and the evolution paths. The performance of SEDMs was assessed by adopting the land cover conversion matrix and connect index.

A. Experimental Datasets

The annual, cloud-free, and spatially seamless classification image set generated from time-series Landsat dataset was utilized to test the performance of the proposed SEDM framework. Details of these two datasets are presented as follows.

Landsat Collection 1 Tiers data (including Level-1 data products generated from Landsat 8 Operational Land Imager (OLI)/Thermal Infrared Sensor (TIRS), Landsat 7 Enhanced Thematic Mapper Plus (ETM+), Landsat 4-5 Thematic Mapper (TM)∗, and Landsat 1-5 Multispectral Scanner (MSS)

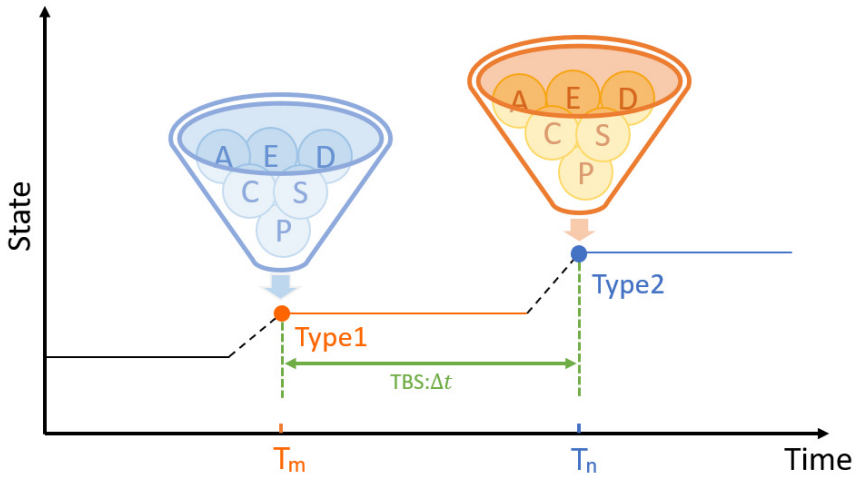

Fig. 6. Sketch map for calculating the evolution timesteps (TBS). T_m and T_n are the time when the two different state types (type1 and type2) are detected, and the time interval (green arrow in the figure) between T_m and T_n is the evolution timesteps. One of the six main state types may appear at both T_m and T_n.

instruments) from June to September were acquired for Shanxi between 1987 and 2018 from the Unite States Geological Survey (https://espa.cr.usgs.gov/) via the Google Earth Engine (GEE) platform. GEE is a cloud-based geospatial analysis platform with massive computational capabilities [50]. The Composite-2-Change approach generated the annual best-available pixel (BAP) image composites by inputting optimal observations for each pixel [51]. The spectral trend analysis was applied to the pixel-level time series of these annual composites to further remove noisy observations (such as haze and unscreened clouds) and infill data gaps (due to missing observations and severe cloud cover) with proxy values [52]. The classification image set was derived from all the spectral bands provided by the Shanxi-wide pixel composites using a random forest classifier available in GEE. In total of 3500 training samples were selected every year to classify land cover classes by the interpretation of high-resolution imagery from Google Earth. The elevation and the slope from the Advanced Spaceborne Thermal Emission and Reflection Radiometer Global Emissivity Database (ASTER-GED) in GEE were assisted in correcting the classification results for higher accuracy. The random sampling method was used in the classification procedure to generate 750 random points each year for verifying the annual classification results. The final land cover maps comprise seven land cover classes, including forest, cropland, grassland, water body, built-up area, mining area, and barren land. The classification accuracy for the individual years has been reported in the appendix. SEDMs were tracked only for state types and their evolution related to the cropland class. The scale of change assessment was determined by the cell size. The cell size was fixed with n = 51 (1.5×1.5 km^2) based on a scale analysis of the indices used in the model and found that the optimal scale is 1.5×1.5 km^2 (51×51). The mean patch fractal dimension, the mean patch area, and the mean patch perimeter were analyzed on ten scales ($n = 11$, 21, 31, 41, 51, 61, 71, 81, 91, and 101). The analysis results show that the optimal scales of mean patch fractal dimension and mean patch area are both 51, and the optimal scale of mean patch perimeter is 61, so the average optimal scale is 51.

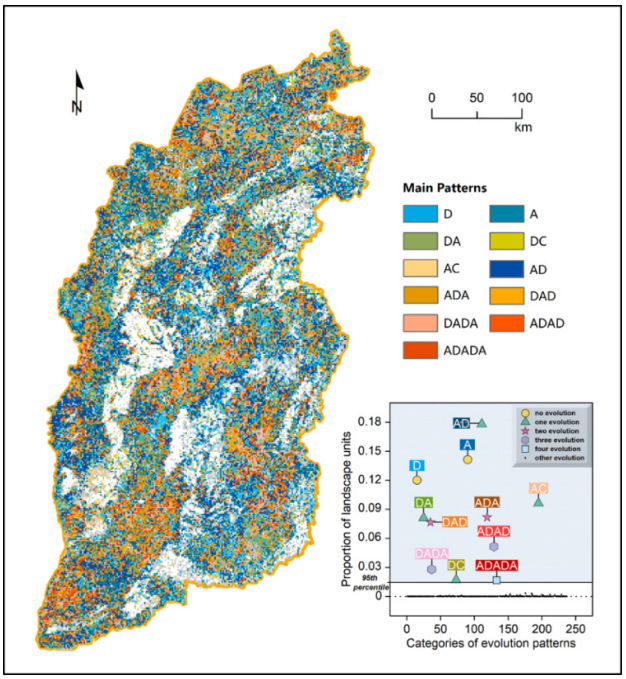

Fig. 7. Map of evolution patterns at the Shanxi site constructed using the SEDM framework. The statistical chart shows the primary patterns between 1987 and 2018.

B. Results of State-Type Evolution Detection

Our experiment presents a sample of the state-type evolution patterns created by SEDMs. Based on this framework, both the evolution patterns in a landscape cell and the overall evolution patterns in the large area can be obtained. At our study site, a total of 233 evolution patterns and 2 "no evolution" patterns occurred over the 31-year span, with the number of evolutions ranging from 0 to 10 (Fig. 7). A total of nine evolutions

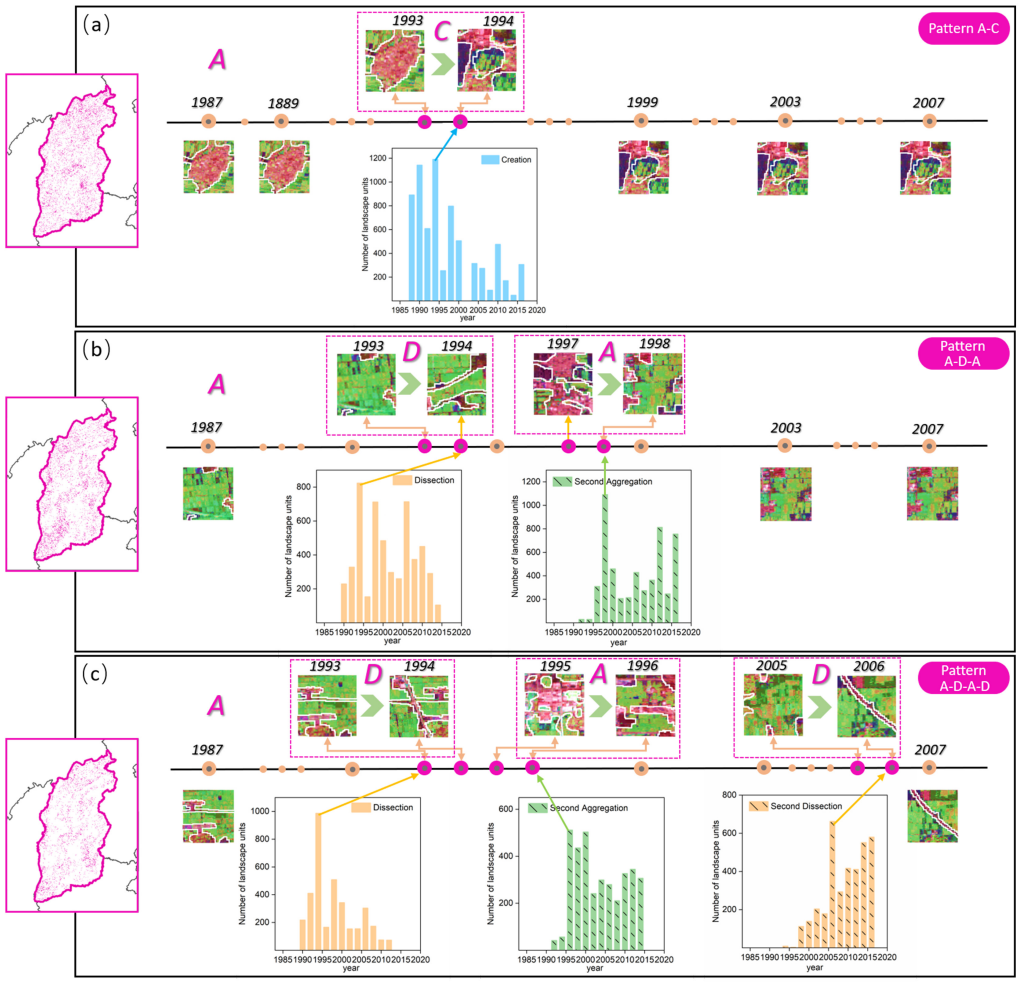

Fig. 8. Evolution time detected in three main evolution patterns. (a) Pattern A-C. (b) Pattern A-D-A. (c) Pattern A-D-A-D. The histogram is a statistic of the number of landscape cells that undergo a type of evolution at the individual years. And the time point connected to the histogram is the most frequent time of this evolution.

dominated the study area (95%), and the largest contributor to evolution patterns was A-D. Considering all the state types, three significant types, A, D, and C, were detected across all landscape cells, while the other types were rarely detected. One reason is that other landscape pattern changes at this site rarely occur, and another reason is that other types are not sensitive to the time scale of cropland landscape pattern changes.

For the performance of detecting evolution time, three main evolution patterns and their evolution times are shown in Fig. 8. The evolution time in each evolution pattern can be analyzed at both the landscape cell and the regional scales. In our experimental cases, the most frequent evolution time from one state type to another in the area that was obtained by calculating the proportions occupied by the evolution time. The evolution time from A to C dominated in 1994. The corresponding evolution time for pattern A-D-A was observed in 1994 and 1998. The evolution of pattern A-D-A-D was primarily detected in 1994, 1996, and 2006. Therefore, the evolution of "to A" mainly occurred in 1996 and 1998; "to D" mainly occurred in 1994 and 2006; "to C" mainly occurred in 1994. SEDMs could also help to analyze the differences in the evolution time between two state types for various evolution patterns. In addition to the mathematical statistics of regional evolution time, the analysis of the temporal and spatial correlations of evolution time could promote the understanding of the regularity in terms of the temporal and spatial changes at regional scale, which could be applied to other similar landscape areas.

The timestep of evolution between two state types was counted by SEDMs across all landscape cells. There were six categories of evolution paths among the nine main detected evolution patterns, including A-C, C-A, A-D, D-A, C-D, and D-C. Fig. 9 shows the corresponding timestep that emerges from these evolution paths. For this experimental case, the TBSs that appear most frequently in these categories are 6 years, 2 years, 2 years, 2 years, 4 years, and 4 years for each category, respectively. The lessons learned from the TSB at the regional scale can promote the prediction of future landscape pattern evolution in larger landscapes.

C. Validity of State-Types Evolution

Although SEDMs are capable of detecting landscape pattern type evolution and evolution time, the reference data used

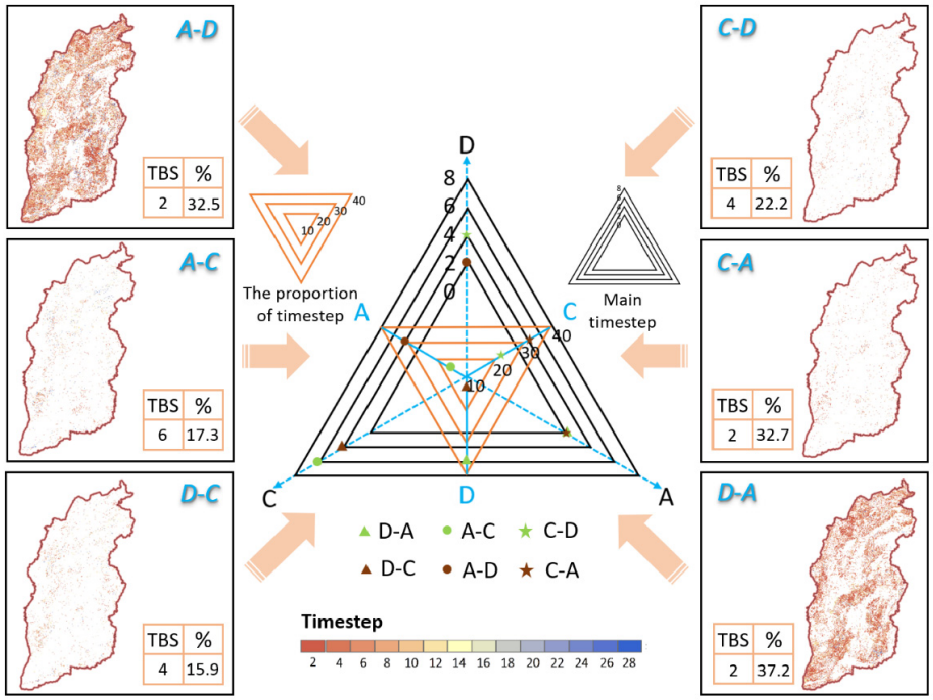

Fig. 9. TBS produced by the SEDM framework for (a) A-D, (b) A-C, (c) D-C, (d) C-D, (e) C-A, and (f) D-A. The data on the black triangle radar chart indicate the timestep with the highest proportion, and the data on the red triangle radar chart indicate the proportion (the largest proportion) of this step. The blue arrow in triangle figure indicates the direction of evolution. For example, the blue arrow in the bottom left corner indicates the evolution from D to C and A to C; the blue arrow in the bottom right corner indicates the evolution from D to A and C to A.

to directly assess its accuracy is hard to acquire. Since the evolution time is the time when a new state is happening, detecting the occurrence of the type, and its time can verify the accuracy of the state-type evolution. To evaluate the accuracy of our framework, the three primary state types and the time they occurred detected by SEDMs were verified using the land cover conversion matrix and connect index based on the state types and were applied over the evolved landscape cells.

Changes in landscape patterns are inseparable from land cover change [2], [53], [54]. The dissection of the agricultural landscape is mainly attributed to the conversion of cultivated land to construction land (such as roads). Therefore, the understanding of the transition of cultivated land at the detected time would contribute to the assessment of type and temporal accuracy. The land cover conversion matrix was calculated before and during the year when state type D occurred to determine whether the landscape cells shifted "from cropland to construction land" at that time. The landscape cells that have the total area of cropland flows into that of construction land in the matrix statistics from the former year to the detected year are referred to as the "accurate cell." This process was assessed for all cells where the SEDM found evolution and were correctly identified in spatial domain. The overall accuracy (OA) was then used to assess the accuracy of the detection results as follows:

$$\mathrm{OA} = \frac{C_d}{C_n} \tag{11}$$

where C_d is estimated as the number of records for which the abovementioned transition occurred in the detected year, and C_n is the total number of cells from C_d containing type D. The OA measure reflects the OA for the detected time and type. The accuracy assessment was performed each year type D was detected. The average OA was 78.27%. The accuracy was particularly high in 1994 (97.18%) and 2006 (84.43%) when type D was detected (Table I).

A benefit of land cover conversion is that it provides robust accuracy estimations for type D and the time that it occurred. However, types A and C are related to many sophisticated cases, in which cropland is transferred. For example, the aggregation and creation of cropland may be caused by the conversion from grassland or forest to cropland, which would lead to inaccurate verification. Therefore, we verified the accuracy of these two state types using the connect index [55], [56], which represents the connection between patches. It was computed considering that each cell exhibits these two types, as follows:

$$\mathrm{CONNECT} = \left[\frac{\sum_{j=k}^{n} C_{ijk}}{\frac{n_i(n_i-1)}{2}}\right] \times 100 \tag{12}$$

where C_{ijk} is a connection between patches j and k; a connection $= 1$ and no connection $= 0$; $\sum_{j=k}^{n} C_{ijk}$ is the number of connections between all patches of type i in the landscape. The connections are calculated by setting the maximum threshold distance to determine whether the patches are connected. If the boundary distance from one patch to another (defined by the 8-neighbor rule) is less than the maximum threshold distance, it indicates that the two patches are connected, otherwise they are not connected. n_i is the number of patches of type i; $(n_i(n_i-1)/2)$ is the number of all possible connections,

TABLE I
VALIDATION RESULTS FOR THREE STATE TYPES

Year	Dissection			Aggregation			Creation		
	Records	Matches	OA(%)	Records	Matches	OA(%)	Records	Matches	OA(%)
1988	2013	1617	80.33	10310	7593	73.65	1281	852	66.51
1990	3915	2989	76.35	6329	5034	79.54	1416	1111	78.46
1992	4270	3474	81.36	3694	3269	88.49	1002	801	79.94
1994	7930	7706	97.18	1290	974	75.50	1891	1550	81.97
1996	1635	1322	80.86	7137	5779	80.97	655	457	69.77
1998	6059	4996	82.46	5866	4198	71.56	1296	779	60.11
2000	3866	2611	67.54	5248	3598	68.56	835	602	72.1
2002	3085	2358	76.43	2215	1349	60.90	1383	793	57.34
2004	2500	1947	77.89	2991	2180	72.89	584	442	75.68
2006	6794	5668	83.43	2851	1920	67.34	655	456	69.62
2008	3630	2522	69.48	1846	1374	74.43	256	180	70.31
2010	4310	3357	77.89	2828	1932	68.32	1626	972	59.78
2012	3782	2981	78.82	3488	2776	79.59	801	614	76.65
2014	2775	2208	79.57	3893	3182	81.74	223	142	63.68
2016	2884	1882	65.26	2065	1583	76.66	737	421	57.12
2017	3804	3056	80.34	4965	3657	73.66	1105	735	66.52
2018	2790	2103	75.38	2636	2097	79.55	1246	977	78.41
Overal accuracy			78.27			74.90			69.65

which represents the number of pairwise connections between all patches of type i, for a defined maximum threshold distance. The CONNECT values with the maximum threshold distance of 500 m between patches were calculated from the program FRAGSTATS v4 [55]

$$\Delta\text{CONNECT} = \text{CONNECT}_t - \text{CONNECT}_{t-1} \tag{13}$$

where CONNECT_t is the value of connectivity at the time when type A or C occurred; CONNECT_{t-1} is the value of connectivity at previous time. Specifically, from the previous year to the detected year for these two state types, the number of nodes between cropland patches increased, and the number of possible nodes decreased for type A, and the number of nodes between cropland patches remained constant, and number of possible nodes increased for type C. As a consequence, if a landscape cell where type A is detected is calculated with $\Delta\text{CONNECT} > 0$, it is an accurate type A cell. Conversely, if the calculated index of the landscape cell is $\Delta\text{CONNECT} < 0$, it is an accurate type C cell. The calculations were performed every year when these two types were detected. Similarly, the final estimation of accuracy could be estimated by the OA, which is obtained by dividing the number of accurate cells by the number of coincident cells of a type. By using our model, the state type and the time achieved relatively high average accuracies in terms of type A ranging from 60.90% to 88.49% and type C ranging from 57.34% to 81.97% (Table I). For the dominant time when type A was detected, the accuracy in 1996 was higher than that in 1988. These validation results from this strategy confirmed that the SEDM framework was effective in extracting CTs' evolution and evolution time using time series land cover data.

IV. DISCUSSION

Holistically characterizing the changes of landscape patterns and their evolution processes across a large area and a long time period is necessary to promote monitoring landscape and reporting activities. SEDMs described here demonstrate a novel framework for generating CTs' evolution maps and detecting evolution time at cell scale using yearly land cover data. Furthermore, it presents an enhanced report of timesteps for mutual transformation of different CTs through the detected evolution time. The strategy validates the effectiveness of the SEDM framework. Landscape pattern changes have been linked to change processes and corresponding drivers [53], [57], [58]. In this coupled human–natural system, the main actual forces that lead to pattern changes in a local landscape come from human's decisions and actions (i.e., agents). The three main state-type results (types A, C, and D) in Shanxi were affected by prior knowledge provided by local agricultural bureau data and farmers' declarations, including agricultural practices (such as reclamation of wasteland), the government policies (such as new countryside construction, freezing of cropland occupied by nonagricultural construction, and grain for green project), and timing

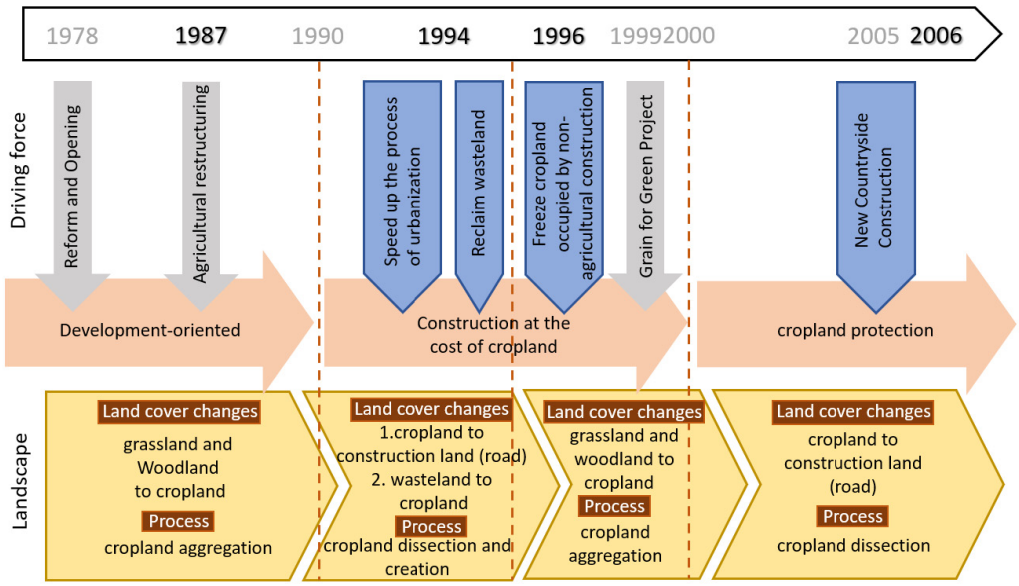

Fig. 10. Basic timeline of policy drivers related to agricultural practices of the Shanxi site and evolution of the landscape. The drivers were provided by local agriculture bureau and identified by a few farmers.

of agricultural development. Overall, the occurrence of state types detected by the SEDM is well explained by the time of government policies and agricultural practices (Fig. 10). In the middle of the 1990s, the "development-oriented agriculture" from local agricultural bureau data was followed by "freezing of cropland occupied by nonagricultural construction" in 1996. According to the survey, during the freezing period, the land for various construction projects could only use the existing construction land, and made full use of wasteland, inferior land, and abandoned land instead of cropland. This force protected cropland and contributed to cropland aggregation. In 1994, the speeding up of the process of urbanization and new countryside construction in 2005 was the efforts taken to add new houses and roads. This resulted in the occurrence of cropland dissection in developing urban and rural areas. Although extensive urbanization was carried out since 1994, as stated by the farmers, the "reclaiming of wasteland" had been operated in many rural areas, which had result in the regaining of some cropland parcels (i.e., the creation of cropland).

Compared with other landscape pattern change-detection models, the three key features of the SEDM framework are summarized as follows.

1) One feature of SEDMs is the comprehensiveness. Landscapes are dynamic ecosystems in which all kinds of change processes are ongoing at any given time, especially managed landscapes. Although some remotely sensed methods have the capacity to detect changes related to one type of landscape pattern change process, the detection of other types that may also have impacts on landscape dynamics remains a vacancy. In contrast to these methods, our framework considers multiple change processes (all of fragmentation, expansion, and aggregation) rather than depending only on a single pattern change type, which may not include the real states of the landscape pattern on the ground. Moreover, our framework allows us to describe landscape patterns after being disturbed by multiple events, not only considering how the fragmentation process changes but also considering the process of aggregation related to recovery from the spatial forms. This is important because some patches are in the processes of fragmentation and reduction, while some may have been aggregated at a certain phase of recovery. Thus, understanding all these processes is needed to better characterize landscape dynamics occurring over time.
2) Another feature is the generality. The framework constitutes an adaptable foundation, which is suitable for landscape monitoring in different applications. More specifically, our conceived patch-tracking mechanism can describe those dynamics through patches coming from different land cover classes of the time series. After the land cover class is determined, the numerous combinations of its attributes (e.g., shape, size, and location) can be analyzed by the model. Note that we did not experiment with all land cover classes during implementation for this simple example. However, our detection would still be implemented once our defined types of pattern changes occurred in the land cover class change. Modifying the combination of land cover class attributes brings some flexibility and the capacity to customize our proposed framework according to the users' tasks. Additionally, the framework defines "evolution" once, depending on the land cover class that is most frequently disturbed by humans and nature. Therefore, it is still valid for other land cover classes to detect the evolution of landscape pattern change process in each landscape cell and larger landscape.

3) Third, we refer to extensibility. With all land cover classes represented as time-space continuous entities, SEDMs provide a simple and flexible approach to landscape pattern monitoring. Depending on the application, the proposed approach can independently generate or transparently combine spatially explicit maps for each state type and timestep. Such maps could then be input into spatially explicit wildlife distribution models or simply used to analyze the structural features of the human footprint (such as cut-block size and frequency distribution) in more detail. The TBS types generated across large areas contributes to calculating a matrix of evolution probabilities between state types, which could be a key function in simulating landscape pattern changes over time (such as the land cover change model and cellular automata model). Furthermore, this framework can generate maps of CT before and after evolution occurs or over any specified time period. The trends of spectral index over time have provided insights into the change processes in various landscapes [59]–[64]. A simultaneous view of state types and current spectral index changes for a given landscape could promote understanding of the relation between landscape patterns and processes, which is a difficult recursive question in landscape ecology. In addition, our framework is capable of integrating agent/individual-based models, an increasingly important way to represent drivers of landscape dynamics. By extrapolating "lessons learned" at data-rich locations to the larger landscape, the SEDM framework can also be explored to design field trials on uncharted areas with an exploratory tool for drawing a global overview of the study site.

However, SEDMs have limitations. First, classification accuracy affects the change detection in landscape pattern. The classification error can bias the calculation of the landscape indices, leading to the misjudgment of state types. In this study, although composite images obtained from all available images can overcome some issues, such as the scan-line corrector failure in Landsat 7, clouds, cloud shadows, and snow, accurate classification in the regions with persistent clouds (such as the south of China) is still a challenge. Reference samples used for modeling and verification are extracted from satellite images through manual interpretation instead of strictly ground truth data. This sample selection process may introduce errors and propagate to the final output. However, in our framework, the absolute accuracy value of classification is not the dominant factors affecting the final outputs, since the recognition of state types is based on the difference between landscape indices from two consecutive land cover maps. Therefore, the result of pattern evolution based on the classification result can be accepted as long as the annual classification accuracy is kept consistent. Second, this framework has room to grow in terms of fully defining state types. Although the method for detection of landscape pattern evolution in experimental sites produced promising detection results, it will omit detection or will not be able to extract the evolution of places with state types outside of the defined types. Some other pattern characteristics of land cover classes (such as position transfer and deformation) in the timing of landscape dynamic change probably prove particularly challenging, and more indices must be considered. Third, we assume that our framework is able to estimate CTs' evolution for all land cover classes, but it may be invalid for the class with more intra-annual variation in some places. The proposed model needs to be improved into a more complex model, if it is to be applied to all cases. Finally, the "one times the types" criterion is set manually based on prior knowledge rather than automatically set. The criteria used in this framework are not universal and are dependent on the actual condition of the study area. Hence, the criteria that automatically adapt to the land cover classes may provide better accuracy. Further work will focus on detecting the state type more intelligently using machine learning or fuzzy theory to capture more comprehensive landscape pattern evolution patterns in a given area, which have great potential in helping policy-makers and land managers to comprehensively report landscape pattern dynamics over large areas.

V. Conclusion

In this article, a novel framework is presented for automatically extracting information on the evolution of landscape pattern changes from annual land cover data. The framework was tested by tracking state types associated with the cropland class in Shanxi, China. The experiments underlined how to deeply explore the main and significant spatial change characteristics from the extracted information at the landscape cell scale that cannot be obtained from previous approaches. The validation based on land cover conversion matrix and connect index indicates that SEDMs can accurately detect CTs and their evolutions, with average OAs of 78.27%, 74.90%, and 69.65% for dissection, aggregation, and creation, respectively. SEDMs differ from previous landscape pattern change detection approaches in three important ways, including the ability to comprehensively characterize landscape pattern changes associated with real change cases for various land cover classes, to reveal the long-term evolution process of state types, and to represent multiple patterns of evolution between pairs of state types. SEDMs can be extended to solve a wide range of issues, including analyzing the relationship between landscape patterns and ecological processes, simulating and predicting ecological processes, and constructing spatiotemporal interaction models. SEDMs describe the change process in more detail, and the combined analysis with ecological process derived from remote-sensing spectrum can get more information of the relationship between landscape pattern and process. Our approach is inherently stochastic, the evolution probability of which can be obtained from timesteps between state types, making it suitable for simulating and predicting changes in landscape patterns. Combined with the time series models, SEDMs can provide a simple and powerful approach for developing various spatiotemporal interaction models.

Acknowledgment

The authors would like to thank the Anonymous Reviewers for providing constructive comments that helped to improve the quality of this article.

REFERENCES

[1] Z. Zheng, S. Du, Y.-C. Wang, and Q. Wang, "Mining the regularity of landscape-structure heterogeneity to improve urban land-cover mapping," *Remote Sens. Environ.*, vol. 214, pp. 14–32, Sep. 2018.

[2] H. Dadashpoor, P. Azizi, and M. Moghadasi, "Land use change, urbanization, and change in landscape pattern in a metropolitan area," *Sci. Total Environ.*, vol. 655, pp. 707–719, Mar. 2019.

[3] C. Liding, L. Yang, L. Yihe, F. Xiaoming, and F. Bojie, "Pattern analysis in landscape ecology: Progress, challenges and outlook," *Acta Ecol. Sinica*, vol. 28, no. 11, pp. 5521–5531, Nov. 2008.

[4] X. Liu, X. Li, Y. Chen, Z. Tan, S. Li, and B. Ai, "A new landscape index for quantifying urban expansion using multi-temporal remotely sensed data," *Landscape Ecol.*, vol. 25, no. 5, pp. 671–682, May 2010.

[5] H. Dadashpoor and F. Salarian, "Urban sprawl on natural lands: Analyzing and predicting the trend of land use changes and sprawl in Mazandaran city region, Iran," *Environ., Develop. Sustainability*, vol. 22, no. 2, pp. 593–614, Feb. 2020.

[6] A. Lausch *et al.*, "Understanding and quantifying landscape structure—A review on relevant process characteristics, data models and landscape metrics," *Ecol. Model.*, vol. 295, pp. 31–41, Jan. 2015.

[7] B. Fu, D. Liang, and N. Lu, "Landscape ecology: Coupling of pattern, process, and scale," *Chin. Geograph. Sci.*, vol. 21, no. 4, pp. 385–391, Aug. 2011.

[8] B. Schröder and R. Seppelt, "Analysis of pattern–process interactions based on landscape models—Overview, general concepts, and methodological issues," *Ecol. Model.*, vol. 199, no. 4, pp. 505–516, Dec. 2006.

[9] R. Hao *et al.*, "Impacts of changes in climate and landscape pattern on ecosystem services," *Sci. Total Environ.*, vol. 579, pp. 718–728, Feb. 2017.

[10] S. Cao, L. Chen, and X. Yu, "Impact of China's Grain for Green Project on the landscape of vulnerable arid and semi-arid agricultural regions: A case study in northern Shaanxi Province," *J. Appl. Ecol.*, vol. 46, no. 3, pp. 536–543, Jun. 2009.

[11] L. Wan, Y. Zhang, X. Zhang, S. Qi, and X. Na, "Comparison of land use/land cover change and landscape patterns in Honghe National Nature Reserve and the surrounding Jiansanjiang Region, China," *Ecol. Indicators*, vol. 51, pp. 205–214, Apr. 2015.

[12] X. Wang, D. Zheng, and Y. Shen, "Land use change and its driving forces on the Tibetan Plateau during 1990–2000," *Catena*, vol. 72, no. 1, pp. 56–66, Jan. 2008.

[13] C. Xu, M. Liu, C. Zhang, S. An, W. Yu, and J. M. Chen, "The spatiotemporal dynamics of rapid urban growth in the Nanjing metropolitan region of China," *Landscape Ecol.*, vol. 22, no. 6, pp. 925–937, May 2007.

[14] X. Zhang, L. Zhou, and Q. Zheng, "Prediction of landscape pattern changes in a coastal river basin in south-eastern China," *Int. J. Environ. Sci. Technol.*, vol. 16, no. 10, pp. 6367–6376, Oct. 2019.

[15] W.-W. Hu, G.-X. Wang, and W. Deng, "Advance in research of the relationship between landscape patterns and ecological processes," *Prog. Geogr.*, vol. 27, no. 1, pp. 18–24, 2008.

[16] W. Kuang, J. Liu, J. Dong, W. Chi, and C. Zhang, "The rapid and massive urban and industrial land expansions in China between 1990 and 2010: A CLUD-based analysis of their trajectories, patterns, and drivers," *Landscape Urban Planning*, vol. 145, pp. 21–33, Jan. 2016.

[17] X. Wang, F. G. Blanchet, and N. Koper, "Measuring habitat fragmentation: An evaluation of landscape pattern metrics," *Methods Ecol. Evol.*, vol. 5, no. 7, pp. 634–646, Jul. 2014.

[18] F. Xiao *et al.*, "Spatio-temporal characteristics and driving forces of landscape structure changes in the middle reach of the Heihe River Basin from 1990 to 2015," *Landscape Ecol.*, vol. 34, no. 4, pp. 755–770, Apr. 2019.

[19] D. Zhou, S. Zhao, and C. Zhu, "The Grain for Green Project induced land cover change in the Loess Plateau: A case study with Ansai County, Shanxi Province, China," *Ecol. Indicators*, vol. 23, pp. 88–94, Dec. 2012.

[20] B. Chen and B. Xu, "A novel method for measuring landscape heterogeneity changes," *IEEE Geosci. Remote Sens. Lett.*, vol. 12, no. 3, pp. 567–571, Mar. 2015.

[21] D. L. Civco, J. D. Hurd, E. H. Wilson, C. L. Arnold, and M. P. Prisloe, Jr., "Quantifying and describing urbanizing landscapes in the Northeast United States," *Photogramm. Eng. Remote Sens.*, vol. 68, no. 10, p. 8, 2002.

[22] Y. Zhang, W. Shen, M. Li, and Y. Lv, "Integrating Landsat time series observations and corona images to characterize forest change patterns in a mining region of Nanjing, eastern China from 1967 to 2019," *Remote Sens.*, vol. 12, no. 19, p. 3191, Sep. 2020.

[23] Y. Han *et al.*, "The growth mode of built-up land in floodplains and its impacts on flood vulnerability," *Sci. Total Environ.*, vol. 700, Jan. 2020, Art. no. 134462.

[24] R. Zhao, Z. Xie, L. Zhang, W. Zhu, J. Li, and D. Liang, "Assessment of wetland fragmentation in the middle reaches of the Heihe River by the type change tracker model," *J. Arid Land*, vol. 7, no. 2, pp. 177–188, Apr. 2015.

[25] J. A. G. Jaeger, "Landscape division, splitting index, and effective mesh size: New measures of landscape fragmentation," *Landscape Ecol.*, vol. 15, pp. 115–130, Feb. 2000.

[26] P. Vogt, K. H. Riitters, C. Estreguil, J. Kozak, T. G. Wade, and J. D. Wickham, "Mapping spatial patterns with morphological image processing," *Landscape Ecol.*, vol. 22, no. 2, pp. 171–177, Jan. 2007.

[27] B. Matsushita, M. Xu, and T. Fukushima, "Characterizing the changes in landscape structure in the Lake Kasumigaura Basin, Japan using a high-quality GIS dataset," *Landscape Urban Planning*, vol. 78, no. 3, pp. 241–250, Nov. 2006.

[28] R. V. O'Neill *et al.*, "Indices of landscape pattern," *Landscape Ecol.*, vol. 1, pp. 153–162, May 1988.

[29] M. Luck and J. G. Wu, "A gradient analysis of urban landscape pattern: A case study from the Phoenix metropolitan region, Arizona, USA," *Landscape Ecol.*, vol. 17, pp. 327–339, Dec. 2002 2002.

[30] M. Herold, J. Scepan, and K. C. Clarke, "The use of remote sensing and landscape metrics to describe structures and changes in urban land uses," *Environ. Planning A, Economy Space*, vol. 34, no. 8, pp. 1443–1458, Aug. 2002.

[31] G. Sanchez-Azofeifa, R. C. Harriss, and D. L. Skole, "Deforestation in Costa Rica: A quantitative analysis using remote sensing imagery," *Biotropica*, vol. 33, pp. 378–384, Sep. 2001.

[32] J. E. Vogelmann, "Assessment of forest fragmentation in southern New England using remote sensing and geographic information systems technology," *Conservation Biol.*, vol. 9, no. 2, pp. 439–449, Apr. 1995.

[33] J. P. Boentje and M. S. Blinnikov, "Post-Soviet forest fragmentation and loss in the green belt around Moscow, Russia (1991–2001): A remote sensing perspective," *Landscape Urban Planning*, vol. 82, no. 4, pp. 208–221, Oct. 2007.

[34] P. D. Pickell, N. C. Coops, S. E. Gergel, D. W. Andison, and P. L. Marshall, "Evolution of Canada's boreal forest spatial patterns as seen from space," *PLoS ONE*, vol. 11, no. 7, Jul. 2016, Art. no. e0157736.

[35] N. C. Coops, S. N. Gillanders, M. A. Wulder, S. E. Gergel, T. Nelson, and N. R. Goodwin, "Assessing changes in forest fragmentation following infestation using time series Landsat imagery," *Forest Ecol. Manage.*, vol. 259, no. 12, pp. 2355–2365, May 2010.

[36] T. Hermosilla, M. A. Wulder, J. C. White, N. C. Coops, P. D. Pickell, and D. K. Bolton, "Impact of time on interpretations of forest fragmentation: Three-decades of fragmentation dynamics over Canada," *Remote Sens. Environ.*, vol. 222, pp. 65–77, Mar. 2019.

[37] R. E. Kennedy *et al.*, "Bringing an ecological view of change to Landsat-based remote sensing," *Frontiers Ecol. Environ.*, vol. 12, no. 6, pp. 339–346, 2014.

[38] C. J. Daniel, L. Frid, B. M. Sleeter, and M. Fortin, "State-and-transition simulation models: A framework for forecasting landscape change," *Methods Ecol. Evol.*, vol. 7, no. 11, pp. 1413–1423, Nov. 2016.

[39] J. Cardille, M. Turner, M. Clayton, S. Gergel, and S. Price, "METALAND: Characterizing spatial patterns and statistical context of landscape metrics," *Bioscience*, vol. 55, pp. 983–988, Nov. 2005.

[40] K. Riitters, J. D. Wickham, R. O'Neill, K. B. Jones, and E. Smith, "Global-scale patterns of forest fragmentation," *Conservation Ecol.*, vol. 4, no. 2, pp. 1–24, 2000.

[41] K. H. Riitters *et al.*, "Fragmentation of continental United States forests," *Ecosystems*, vol. 5, pp. 815–822, Dec. 2002.

[42] D. A. Saunders, R. J. Hobbs, and C. R. Margules, "Biological consequences of ecosystem fragmentation—A review," *Conservation Biol.*, vol. 5, pp. 18–32, Mar. 1991.

[43] N. O. Soverel, N. C. Coops, J. C. White, and M. A. Wulder, "Characterizing the forest fragmentation of Canada's national parks," *Environ. Monitor. Assessment*, vol. 164, nos. 1–4, pp. 481–499, May 2010.

[44] L. Mosaics, *The Ecology of Landscapes and Regions*. Cambridge, U.K.: Cambridge Univ., 1995.

[45] E. H. Wilson, J. D. Hurd, D. L. Civco, M. P. Prisloe, and C. Arnold, "Development of a geospatial model to quantify, describe and map urban growth," *Remote Sens. Environ.*, vol. 86, no. 3, pp. 275–285, Aug. 2003.

[46] R. Forman, "Land mosaics: The ecology of landscapes and regions (1995)," in *The Ecological Design and Planning Reader*. Washington, DC, USA: Island Press, 2014, pp. 217–234.

[47] D. R. Patton, "A diversity index for quantifying habitat 'edge,"' *Wildlife Soc. Bull.*, vol. 3, no. 4, pp. 171–173, 1975.
[48] M. Game, "Best shape for nature reserves," *Nature*, vol. 287, no. 5783, pp. 630–632, Oct. 1980.
[49] X. Li *et al.*, "The adequacy of different landscape metrics for various landscape patterns," *Pattern Recognit.*, vol. 38, no. 12, pp. 2626–2638, Dec. 2005.
[50] N. Gorelick, M. Hancher, M. Dixon, S. Ilyushchenko, D. Thau, and R. Moore, "Google Earth engine: Planetary-scale geospatial analysis for everyone," *Remote Sens. Environ.*, vol. 202, pp. 18–27, Dec. 2017.
[51] T. Hermosilla, M. A. Wulder, J. C. White, N. C. Coops, and G. W. Hobart, "Updating Landsat time series of surface-reflectance composites and forest change products with new observations," *Int. J. Appl. Earth Observ. Geoinf.*, vol. 63, pp. 104–111, Dec. 2017.
[52] T. Hermosilla, M. A. Wulder, J. C. White, N. C. Coops, and G. W. Hobart, "An integrated Landsat time series protocol for change detection and generation of annual gap-free surface reflectance composites," *Remote Sens. Environ.*, vol. 158, pp. 220–234, Mar. 2015.
[53] H. Dadashpoor and M. Alidadi, "Towards decentralization: Spatial changes of employment and population in Tehran Metropolitan Region, Iran," *Appl. Geogr.*, vol. 85, pp. 51–61, Aug. 2017.
[54] P. Netzel and T. F. Stepinski, "Pattern-based assessment of land cover change on continental scale with application to NLCD 2001–2006," *IEEE Trans. Geosci. Remote Sens.*, vol. 53, no. 4, pp. 1773–1781, Apr. 2015.
[55] K. McGarigal, S. Cushman, and E. Ene, "FRAGSTATS v4: Spatial pattern analysis program for categorical and continuous maps," Univ. Massachusetts, Amherst, MA, USA, 2012. [Online]. Available: https://www.umass.edu/landeco/research/fragstats/fragstats.html
[56] A. G. Spanowicz and J. A. G. Jaeger, "Measuring landscape connectivity: On the importance of within-patch connectivity," *Landscape Ecol.*, vol. 34, no. 10, pp. 2261–2278, Oct. 2019.
[57] L. S. Bertolo, G. T. N. P. Lima, and R. F. Santos, "Identifying change trajectories and evolutive phases on coastal landscapes. Case study: São Sebastião Island, Brazil," *Landscape Urban Planning*, vol. 106, pp. 115–123, May 15 2012.
[58] J. Solon, "Spatial context of urbanization: Landscape pattern and changes between 1950 and 1990 in the Warsaw metropolitan area, Poland," *Landscape Urban Planning*, vol. 93, nos. 3–4, pp. 250–261, Dec. 2009.
[59] H. Yin *et al.*, "Monitoring cropland abandonment with Landsat time series," *Remote Sens. Environ.*, vol. 246, Sep. 2020, Art. no. 111873.
[60] M. A. Wulder *et al.*, "Current status of Landsat program, science, and applications," *Remote Sens. Environ.*, vol. 225, pp. 127–147, May 2019.
[61] M. E. Andrew and H. Warrener, "Detecting microrefugia in semi-arid landscapes from remotely sensed vegetation dynamics," *Remote Sens. Environ.*, vol. 200, pp. 114–124, Oct. 2017.
[62] I. Nitze and G. Grosse, "Detection of landscape dynamics in the Arctic Lena Delta with temporally dense Landsat time-series stacks," *Remote Sens. Environ.*, vol. 181, pp. 27–41, Aug. 2016.
[63] K. S. Willis, "Remote sensing change detection for ecological monitoring in United States protected areas," *Biol. Conservation*, vol. 182, pp. 233–242, Feb. 2015.
[64] Z. Zhu, "Change detection using Landsat time series: A review of frequencies, preprocessing, algorithms, and applications," *ISPRS J. Photogramm. Remote Sens.*, vol. 130, pp. 370–384, Aug. 2017.

Lingwen Tian received the M.S. degree in surveying engineering from the China University of Geosciences, Beijing, China, in 2018, where she is pursuing the Ph.D. degree in surveying science and technology.

Her research interests include environmental remote sensing and remote-sensing time series analysis.

Xiangnan Liu received the B.S. degree in geography from Hunan Normal University, Changsha, China, in 1987, and the M.S. and Ph.D. degrees in remote sensing and geographic information system from Northeast Normal University, Changchun, China, in 1990 and 1996, respectively.

In 1990, he joined the Faculty of Northeast Normal University. Since 2006, he has been a Professor with the School of Information Engineering, China University of Geosciences, Beijing, China. He has authored 7 books and more than 100 articles. His research interests include modeling, quantitative analysis of natural resources, ecological, and environmental systems by remote sensing, GIS, and geostatistics.

Meiling Liu received the B.S. degree from Hunan Normal University, Changsha, China, in 2002, and the M.S. and Ph.D. degrees from the China University of Geosciences, Beijing, China, in 2006 and 2011, respectively.

She is an Associate Professor with the School of Information Engineering, China University of Geosciences. Her research interests include developing the models and methods into studies of natural resources, ecological, and environmental systems by remote sensing and GIS.

Ling Wu recevied the B.S. degree in geographic information system and the M.S. and Ph.D. degrees in cartography and geographic information engineering from the China University of Geosciences, Beijing, China in 2007, 2010, and 2013, respectively.

He has been a Post-Doctoral Researcher with the Institute of Remote Sensing and GIS, Peking University, Beijing, from 2013 to 2016. He is an Associate Professor with the School of Information Engineering, China University of Geosciences, Beijing. His research interests include time series analysis and scale transformation of remote-sensing products.